

# We are IntechOpen, the world's leading publisher of Open Access books Built by scientists, for scientists

4,900

Open access books available

123,000

International authors and editors

140M

Downloads

Our authors are among the

154

Countries delivered to

TOP 1%

most cited scientists

12.2%

Contributors from top 500 universities



WEB OF SCIENCE™

Selection of our books indexed in the Book Citation Index  
in Web of Science™ Core Collection (BKCI)

Interested in publishing with us?  
Contact [book.department@intechopen.com](mailto:book.department@intechopen.com)

Numbers displayed above are based on latest data collected.  
For more information visit [www.intechopen.com](http://www.intechopen.com)



# In Situ Titanium Composites: XRD Study of Secondary Phases Tied to the Processing Conditions and Starting Materials

*Eva María Pérez-Soriano, Cristina M. Arévalo-Mora  
and Isabel Montealegre-Meléndez*

## Abstract

Nowadays, the development of high specific modulus materials involves studies of new materials and novel manufacturing routes. From the point of view of composite materials, titanium composites (TMCs) have been long studied for their interesting properties, as a result of the conjunction of low-density and high mechanical properties, as well as corrosion resistance. Among various processing techniques, the in situ reinforced method shows many advantages above the rest. The reactions between matrix and reinforcement drive up the final properties of TMCs. Varying the processing conditions, in addition to reinforcement type and content, significant variations are expected in TMCs' behaviour. In this regard, the present study draws on previous author works. The specimens studied were manufactured by hot consolidation processes, inductive hot pressing (iHP) and direct hot pressing (DHP), at different operational parameters and compositions. X-ray powder diffraction (XRD) investigations tied formations of secondary phases to substantive changes in TMC behaviour under the influence of the fabrication parameters.

**Keywords:** XRD analysis, titanium composites, secondary phases, in situ reaction, matrix strengthening

## 1. Introduction

Over the last decades, investigations about composite materials have made great advances in understanding the importance of the starting materials and the manufacturing process, for the development of novel materials with outstanding properties [1]. In this regard, in the field of metal matrix composites, research studies have been conducted to achieve optimal bounding matrix reinforcement, improving the strength of the metal matrix composites (MMCs) [2]. Light metal matrix composites are valued, particularly in certain applications where low density should be balanced with mechanical requirements [3]. In particular, titanium composites (TMCs) offer these advantages over other light metal matrices [1, 4]. Their good corrosion behaviour and high specific properties make TMCs one of the most suitable candidates for aerospace applications [5].

Several authors have described several classifications of these materials. One of these classifications could be considered based on the kind of reinforcements: continuous or discontinuous reinforcement [6, 7]. Other classifications could be done according to the manufacturing route: traditional methods or powder metallurgy techniques [8–12]. An interesting route to promote the strengthening of the matrix is the “in situ” formation of secondary phases. This method allows a clean and well bounding between the matrix and the reinforcement [9]; consequently, better final behaviour of the TMCs may be expected [13, 14].

On the basis of previous and recent studies, this work focuses on TMCs which were manufactured employing discontinuous ceramic reinforcement. These ceramic phases were selected according to their reactivity with the titanium matrix. Many authors show the great variety of ceramic reinforcements; however, in this investigation TiC, TiB<sub>2</sub>, B, and B<sub>4</sub>C particles were studied. They were considered as precursors of secondary phase formation by in situ techniques [15–20].

From the manufacturing process point of view, powder metallurgy techniques of hot consolidation have proved useful at the study of in situ composites [21]. Therefore, for the development of TMCs, inductive hot pressing has been selected among other manufacturing processes. The experience of the authors in this technique had led to laying the basis of this study [22–28].

By a thorough analysis of the properties of the produced specimens via inductive hot pressing at different temperatures by the use of several starting material compositions, specific features of the TMCs could be studied. In this regard, the employment of the XRD technique is crucial in understanding the reaction phenomena between the matrix and the reinforcement. Furthermore, the behaviour of the ceramic particles in the matrix could be unpredictable and variable depending upon many factors; this study is the main objective to analyse the phenomena that could occur when factors as starting powder composition and processing parameters are varied and ultimately how these factors affect the final properties of the TMCs.

## **2. Materials and methods**

The interest in understanding the influence of the starting materials on the final behaviour of TMCs motivated the study of three ceramic materials as reinforcements testing various concentrations in titanium matrices. Hence, for the TMC manufacture, diverse starting blends were prepared. The innovation of this investigation lies in the phase analysis carried out in specimens made from these blends. The employment of several operation temperatures and reinforcement typologies and concentrations allowed for the searching of significant differences, among the fabricated TMCs, while all these specimens have been processed at similar processing conditions.

The titanium grade 1 employed was manufactured by TLS GmbH (Bitterfeld, Germany). This titanium powder showed a spherical morphology and D<sub>50</sub> below 45 μm. The four ceramic reinforcements were chosen considering their reactive behaviour in respect of the secondary phases’ formation in titanium matrices. The supplier for TiC powder was H.C. STARK GmbH (Goslar, Germany) and for B<sub>4</sub>C powders was abcr GmbH (Karlsruhe, Germany), and the company for TiB<sub>2</sub> was Treibacher Industrie AG (Althofen, Austria). The characterization of all the powders was carried out to verify the manufacturers’ data about their size and morphology. The particle size distribution of the powders was measured by laser diffraction analysis (Mastersizer 2000, Malvern Instruments, Malvern, United Kingdom); these results are shown in **Table 1**.

X-ray powder diffraction analysis was done using a Bruker D8 Advance A25 (Billerica, Massachusetts, United States of America) with Cu-K<sub>α</sub> radiation for the phase characterisation of as-received Ti, TiC, TiB<sub>2</sub>, and B<sub>4</sub>C powders and studying

Material	Morphology	D <sub>50</sub> (μm)
Ti	Spherical	29.05
TiC	Faceted	4.9
TiB <sub>2</sub>	Irregular	4.76
B <sub>4</sub> C	Faceted	63.76

**Table 1.**  
 Characteristics of the starting materials.

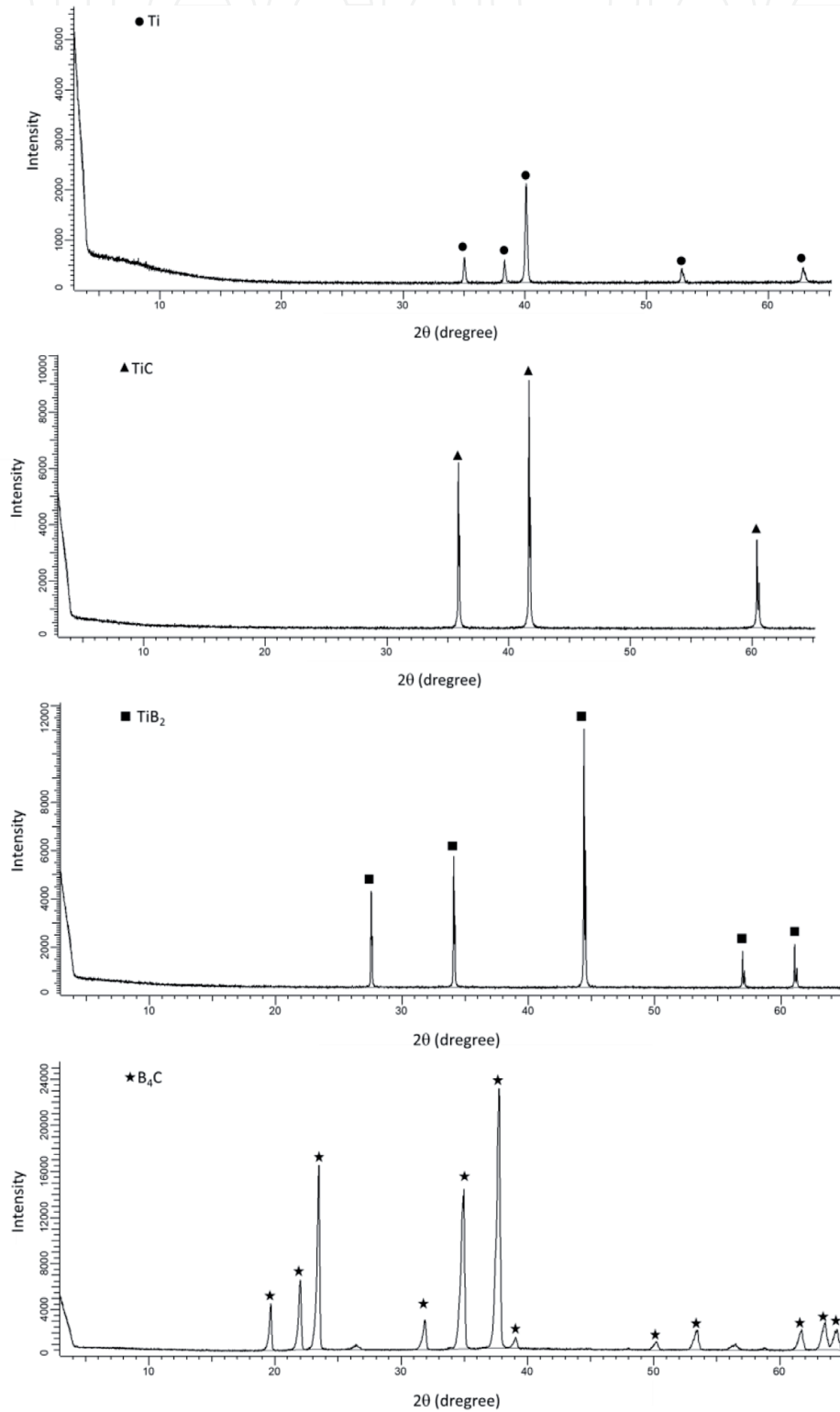


**Figure 1.**  
 XRD analysis of the starting powders: Ti grade 1, TiC, TiB<sub>2</sub>, and B<sub>4</sub>C.

the phase evolution of sintered TMCs. The reference intensity ratio (RIR) analysis was performed to semi-quantitatively determine the phases. This method is based on setting the diffraction data to the diffraction of standard reference materials. The intensity of a diffraction peak profile is a convolution of diverse factors, being the most representative of the concentration of the analysed species.

In **Figure 1**, the X-ray diffraction spectra of the starting materials (as-received) are shown. Based on the obtained diffraction patterns, these materials consist of only Ti, TiC, TiB<sub>2</sub>, and B<sub>4</sub>C, respectively.

Previously in the TMC consolidation, the raw material blends were prepared according to the fixed percentages in volume (see **Table 2**). The mixing procedure was described in previous authors' work [28]. Next, the specimens were sintered. To consolidate the TMCs, a self-made hot pressing machine, inductive hot pressing (iHP) equipment of RHP-Technology GmbH & Co. KG (Seibersdorf, Austria), was used. This machine enabled the operational cycle time to be reduced thanks to its advantageous high heating rate, which in turn is due to its special inductive heating setup. The prepared powders were inserted in the graphite die; it was lined with thin graphite paper and a protective coating of boron nitride (BN). The same procedure and die were used for all the iHP cycles (punch Ø 20 mm). Methods based on this rapid hot consolidation are considered as preferred techniques for in situ fabrication of nearly fully dense TMCs [29]. In **Table 2**, the processing conditions are shown. Likewise, the curves of the process cycle are represented graphically in

Ti matrix and reinforcement		Processing parameters		
Reinforcement material	Volume [%]	Temperature [°C]	Time [min]	Pressure [MPa]
TiC	10, 20, 30	1000, 1100, 1200	15	50
TiB <sub>2</sub>	10, 20, 30	1000, 1100, 1200	15	50
B <sub>4</sub> C	10, 20, 30	1000, 1100, 1200	15	50

**Table 2.**  
Reinforcement percentages and processing parameters.

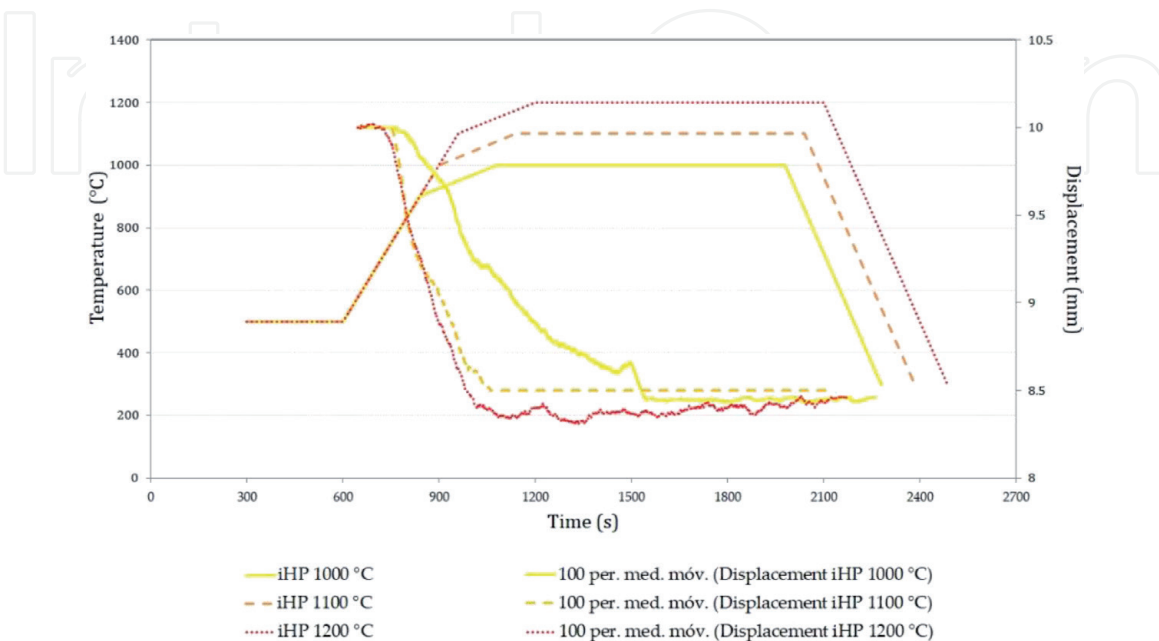


**Figure 2.**  
Diagram of the inductive hot-pressing cycle: time vs. temperature and piston displacement.



**Figure 2.** The iHP equipment worked in vacuum conditions ( $5 \cdot 10^{-4}$  bar), the cycle heating rate being  $50^\circ\text{C}/\text{min}$ . Following the consolidation, the specimens were dislodged from the graphite die and cut in half vertically.

After a thorough metallographic preparation on the cross section of the specimens, the X-ray analysis and the microstructural study were performed. It was studied by means of SEM, using JEOL 6460LV (Tokyo, Japan) and FEI Teneo (Oregon, United States of America). Furthermore, the hardness measurement was carried out; seven indentations were performed on each specimen, avoiding the ceramic particles. A tester model, Struers Duramin A300 (Ballerup, Denmark), was employed to ascertain the Vickers hardness (HV2). An ultrasonic method (Olympus 38DL, Tokyo, Japan) was employed to calculate the Young modulus by measuring longitudinal and transversal propagation velocities of acoustic waves [30]. Archimedes' method (ASTM C373-14) was set for the density measurement.

### 3. Results and discussions

#### 3.1 X-ray diffraction analysis and microstructural study

This section has been structured according to the employed reinforcement, in order to present the results and to perform their discussion clearly and concisely. Therefore, there have been three subparts taking into account the ceramic materials used as starting reinforcements in the TMC manufacturing.

##### 3.1.1 TiC

The X-ray diffraction spectra of TMCs made from TiC-Ti blends are shown in **Figure 3**. Based on the obtained diffraction patterns, these materials consist of Ti and  $\text{TiC}_x$  phases. On the one hand, the X-ray analysis reveals that there are only Ti and TiC phases in specimens produced at  $1000^\circ\text{C}$ , regardless of whether the highest or the lowest TiC concentration (vol.%) was used in the starting blend. Likewise, only TiC stoichiometric phase is detected in specimens made from 10 vol.% of TiC, even in specimens produced at  $1100$  and  $1200^\circ\text{C}$ . On the other hand, the peak intensity of the Ti phase decreased; meanwhile, there was an apparition of slight diffraction peaks of nonstoichiometric TiC phase named  $\text{TiC}_{0.67}$ . It suggested that there were possible reactions between the Ti and diffused C from the TiC particles at high concentrations (20 vol.% TiC and 30 vol.% TiC). The intensification of the nonstoichiometric TiC peaks from  $1100$  to  $1200^\circ\text{C}$  indicates the increase in the volume fraction of this phase, which can be confirmed by the RIR semi-quantification analysis. The results from RIR analysis are shown in **Table 3**. These results may lead to the assumption that the phenomenon of C diffusion was more significant at the highest TiC concentration (30 vol.%) and the highest operational temperature ( $1200^\circ\text{C}$ ). In agreement with the values of the RIR semi-quantification analysis in **Table 3**, the higher the TiC in starting materials was used, the higher the TiC phase values in the RIR analysis was detected.

To clarify the distribution of the nonstoichiometric  $\text{TiC}_x$  phases in TMCs, energy-dispersive X-ray spectroscopy (EDS) analysis was performed. In **Figure 4**, the EDS result revealed that there were concentration gradients between the centres of the TiC particles and the matrix. This clearly demonstrated the value of the temperature and the starting material compositions as influencing factors in the final behaviour of the TMCs. Moreover, it can be observed from **Figure 4** that C was diffused in the region, which is rich in titanium. This is in accordance with the slight displacement of the Ti peaks in the TMC patterns when the specimens were consolidated especially at  $1200^\circ\text{C}$ .

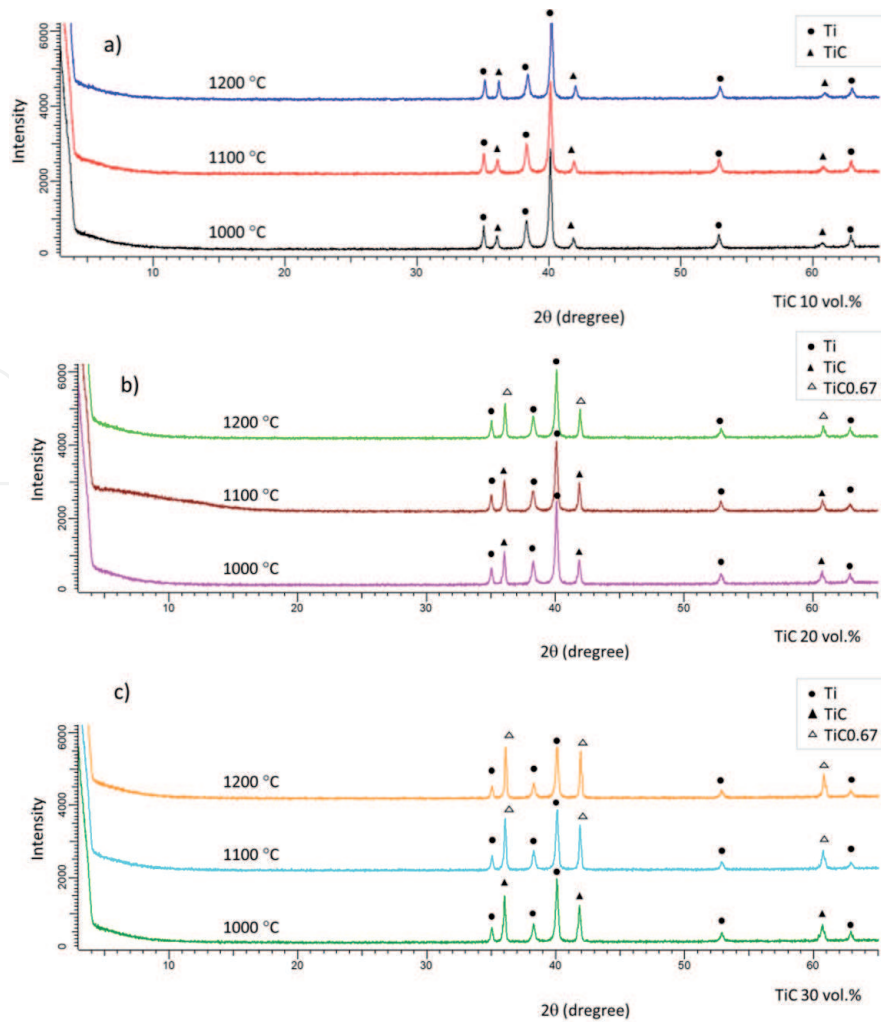


**Figure 3.** XRD patterns of TMCs reinforced using (a) 10 vol.% of TiC, (b) 20 vol.% of TiC and (c) 30 vol.% of TiC.

Temperature (°C)	vol.%	Ti (%)	TiC (%)	TiC <sub>0.67</sub> (%)
1000	10	97.8	2.2	
	20	96.3	6.4	
	30	88.5	11.5	
1100	10	96.9	3.1	
	20	91.9	8.1	
	30	84.4		15.6
1200	10	94.6	3.6	1.8
	20	91.4		8.6
	30	81.0		19.0

**Table 3.** Reinforcement percentages and processing parameters.

From the microstructural point of view, there were several differences observed in the specimens, which depended not only on the processing temperature employed but also on the starting reinforcement concentration. In this regard, the lower the concentration of TiC (10 vol.%), the fewer the pores observed in the TMC microstructure. Moreover, some agglomerations of the TiC particles could be clearly appreciated in specimens made from the blend with 30 vol.% of TiC; there are little pores observed

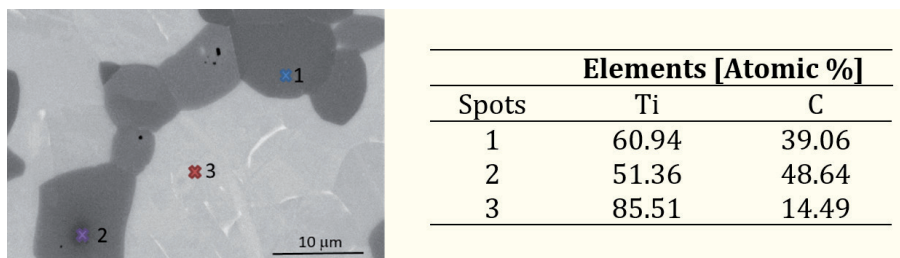


**Figure 4.** On the left, SEM image of TMCs processed at 1200°C, with starting TiC composition of 20 vol.%. On the right, EDX analysis of three spots on the cross section of such TMC.

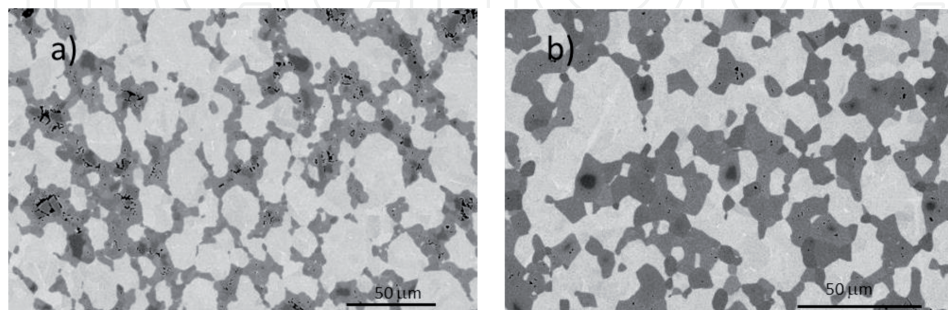


**Figure 5.** SEM images of TMCs made from composition of 30 vol.% of TiC hot consolidated at (a) 1000°C and (b) 1200°C.

in the centre of these ceramic particles' agglomerations in the titanium matrices (**Figure 5a**). The pores tended to close with the increase in temperature. In line with the diffusion phenomenon mentioned above, a possible reason for the porous reduction may be the diffusion of the C element and, consequently, the formation of  $TiC_x$  phases. Furthermore, the cited pores could also be caused by material removal during the metallographic preparation, which suggested that major bonding between TiC particles and the matrix decreases the material removal. It indicates that the reaction between the C sourced by TiC particles and Ti from the matrix involved a strong interfacial bonding. Therefore, the rising of the temperature benefited, and it was very useful to obtain major densification. It is worth noting that the reinforcement agglomeration could be a problem as a barrier for affecting the diffusion phenomenon and the interfacial contact. For that reason, the pores are only observed in the centre of the mentioned agglomerations (see **Figure 5**).

### 3.1.2 $TiB_2$

**Figure 6** shows the XRD patterns of the TMCs reinforced with  $TiB_2$  particles. In this respect, particular attention will be devoted to the existence of peaks of  $Ti_3B_4$ , while there was an increment of the temperature from 1100 to 1200°C. Likewise, it can be seen that the XRD patterns of the specimens produced at 1000°C only contain strong diffraction peaks of  $TiB_2$  phase and slight diffraction peaks of TiB phase. The  $Ti_3B_4$  peaks appear independently of the starting  $TiB_2$  concentration (vol.%), being only related to the processing temperature (1100 and 1200°C).

**Table 4** shows the semi-quantification analysis of the TMCs reinforced by  $TiB_2$  particles. As many authors describe [9, 12, 13, 16, 19, 22, 29], there are reactions between B from  $TiB_2$  particles and the Ti matrix, resulting in the in situ TiB phase. Thus, it would be expected that the percentages of in situ TiB phase were proportional to the initial composition of  $TiB_2$  in the starting blend. However, observing the values presented in **Table 4**, the key parameter was the temperature instead of the concentration,



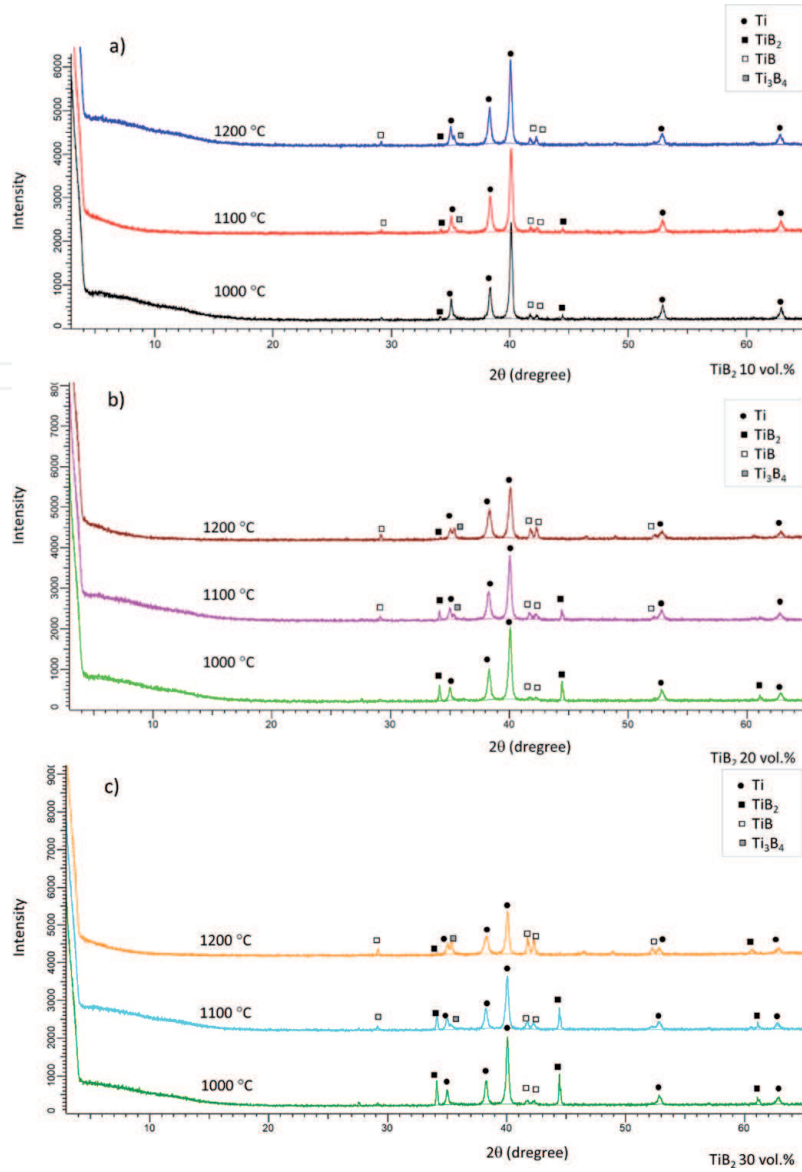


**Figure 6.** XRD patterns of TMCs reinforced in the starting blend with (a) 10 vol.% of  $TiB_2$ , (b) 20 vol.% of  $TiB_2$ , and (c) 30 vol.% of  $TiB_2$ .

Ti matrix and $TiB_2$					
Temperature [°C]	vol.%	Ti (%)	$TiB_2$ (%)	TiB	$Ti_3B_4$ (%)
1000	10	91.3	4.7	4.0	
	20	78.2	19.0	2.8	
	30	68.3	28.1	2.9	
1100	10	90.2	4.1	3.9	1.8
	20	77.9	12.0	6.8	3.3
	30	65.0	24.8	7.4	2.8
1200	10	88.5	2.5	6.2	2.6
	20	76.7	3.9	12.3	7.1
	30	72.9	3.5	20.9	3.4

**Table 4.** RIR semi-quantification analysis of TMCs made from Ti- $TiB_2$  blends, manufactured at different temperatures (by iHP).

promoting the apparition of TiB as in situ formed phase. Owing to the rising temperature, the diffusion mechanism was driven by the temperature increments of 100°C (from 1000 to 1100°C and from 1100 to 1200°C). The highest temperature (1200°C) played a major role in the formation of TiB, independently of the operational temperature. Obviously, at the same temperature, there was more TiB detected in specimens made from starting powder with the higher TiB<sub>2</sub> composition (30 vol.% of TiB<sub>2</sub>).

Microstructural study of these TMCs confirmed the visual existence of the in situ TiB<sub>x</sub> phases. Moreover, some pores were detected in areas where the TiB<sub>2</sub> particles were slightly agglomerated. As mentioned in the results of the microstructural analysis of TMC reinforced by TiC<sub>x</sub> phases, the referred pores were located in the centre of particle agglomeration. The higher the concentration of particles and the lower the operational temperature, the more significant the apparition of pores in the TMCs. In **Figure 7**, the commented pores can be recognized.

The influence of the temperature was relevant once again to close these pores, as in similitude with the TiC. Many studies [31] attempted to show the importance of strong bonding between the matrix and the TiB<sub>x</sub> phases; the no contact between the reinforcement and the matrix, in addition to the inappropriate processing temperature, inhibited the formation of in situ secondary phases. By increasing the operational temperature, improvement in the diffusion phenomenon was expected.

SEM images of the microstructure of TMCs processed at 1100°C are shown in **Figure 8**. The results about homogenous distribution and increase in the volume of reinforcements in the Ti matrix are in accordance to the RIR analysis. In **Figure 8a**, the reinforcements on the matrix can be easily recognized. Observing the microstructural evolution by increment of the composition, the smaller TiB<sub>2</sub> particles were surrounded by the in situ formed phases when the starting composition of TiB<sub>2</sub> was the lowest. However, in **Figure 8c**, coarse TiB<sub>2</sub> particles were also surrounded by phases with minor size.

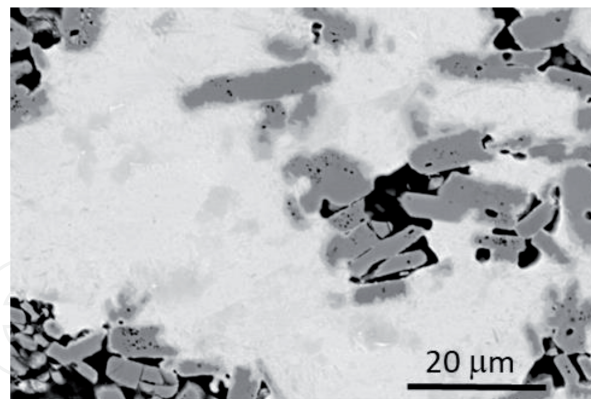


**Figure 7.**  
*SEM image of TMC reinforced with 30 vol.% of TiB<sub>2</sub> particles consolidated at 1000°C.*

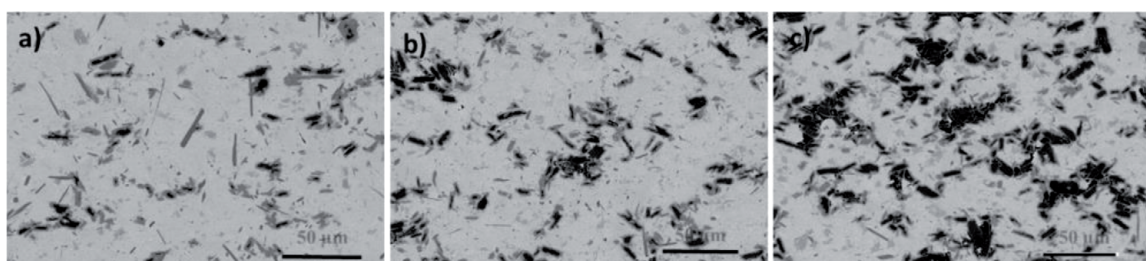
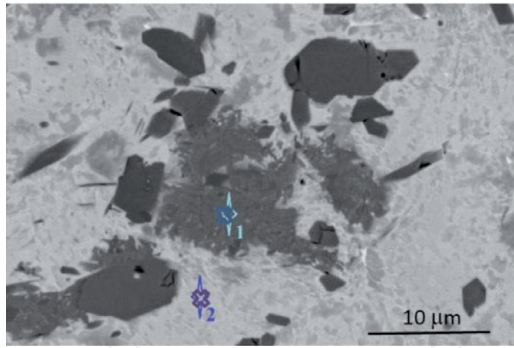


**Figure 8.**  
*SEM images of TMCs processed at 1100°C with different percentages of TiB<sub>2</sub> in the starting blends: (a) 10 vol.%, (b) 20 vol.%, and (c) 30 vol.%.*



Elements [Atomic %]		
Spots	Ti	B
1	33.93	66.07
2	55.05	44.95

**Figure 9.** SEM image of TMC with 10 vol.% of  $TiB_2$  in the starting blend, processed at  $1200^\circ C$ .

The rising in temperature was crucial for reactions between the matrix and the  $TiB_2$  particles. At  $1200^\circ C$ , there were major diffusion of B through the matrix and more formation of the in situ  $TiB_x$  phases. **Figure 9** shows two different areas on a cross section (iHP at  $1200^\circ C$ ), where the B distribution varied considerably; the darkest region in the centre corresponds with the highest concentration of B. It suggests that the dark grey areas were originally the  $TiB_2$  particles, which were surrounded by the in situ  $TiB_x$  phases.

### 3.1.3 $B_4C$

The use of  $B_4C$  offers considerable scope for diversification and development of in situ secondary phases (TiC and TiB). Hence, a wide range of studies intended to demonstrate the suitability of  $B_4C$  as a source of B and C for in situ secondary phases, owing to its reactive behaviour with the Ti matrix. The  $B_4C$  particles can trigger reactions whose products contribute to enhance the TMC properties. In this regard, TiC and TiB phases may expect to be observed and analysed in this type of TMCs. **Figure 9** shows the XRD patterns of the TMCs reinforced with  $B_4C$  particles. It can be verified that the highest temperature of the iHP process and the holding time (15 minutes) were insufficient for a full reaction between the boron carbide particles and the titanium matrices, even at the lowest concentration of  $B_4C$ . Thus, this fact occurred independently of the starting compositions, confirmed by the

Ti matrix and $B_4C$					
Temperature [ $^\circ C$ ]	$B_4C$ vol.%	Ti (%)	$B_4C$ (%)	TiB (%)	TiC (%)
1000	10	92.2	5.7	1.6	0.5
	20	86.4	10.8	1.8	1.0
	30	78.0	18.3	2.2	1.5
1100	10	90.6	5.7	2.7	1.0
	20	81.2	10.3	6.5	2.0
	30	73.3	17.9	6.5	2.3
1200	10	89.0	4.9	5.0	1.1
	20	80.6	10.0	7.0	2.3
	30	64.4	17.1	14.3	4.2

**Table 5.** RIR semi-quantification analysis of TMCs made from Ti- $B_4C$  blends, manufactured at different temperatures (by iHP).

existence of peaks related to the boron carbide. Likewise, there were observed peaks matching TiB and TiC patterns.

The intensification of TiB and TiC peaks from 1000 to 1200°C reflects the increase in the volume fraction of these phases, which can also be seen in the RIR analysis shown in **Table 5**.

The microstructural study shows the homogenous dispersion of the B<sub>4</sub>C particles in the matrix. In this context, there were no agglomerations visually detected. This suggests that there was no porosity related to particles agglomerations as commented previously in TMCs reinforced by TiB<sub>2</sub> and TiC. It could be considered as an advantage of the B<sub>4</sub>C as reinforcement in comparison with other ceramic particles. **Figure 11** shows TMCs processed at the same temperature with different B<sub>4</sub>C percentages.

Regarding the processing temperature, there were significant differences related to the reaction between the matrix and the B and C from the B<sub>4</sub>C particles. At the lowest temperature (1000°C), the formation of the in situ TiB and TiC phases was proportional to the starting content of B<sub>4</sub>C. Employing 10 vol.% of B<sub>4</sub>C, small proportions of in situ phases were detected (see **Table 5**). However, increasing the temperature to 1100°C and using 10 vol.% of B<sub>4</sub>C, the percentage of in situ TiC phase doubled its value, also, by the employment of 20 and 30 vol.%. This is in agreement with the intensity of the peaks of this phase in the TMC patterns (**Figure 10**). As expected, the major in situ formation of secondary phases took place at 1200°C.

**Figure 12** reveals how the in situ phases surrounded the B<sub>4</sub>C particles, being a reaction layer clearly defined. Obviously, the higher the starting B<sub>4</sub>C composition, the more

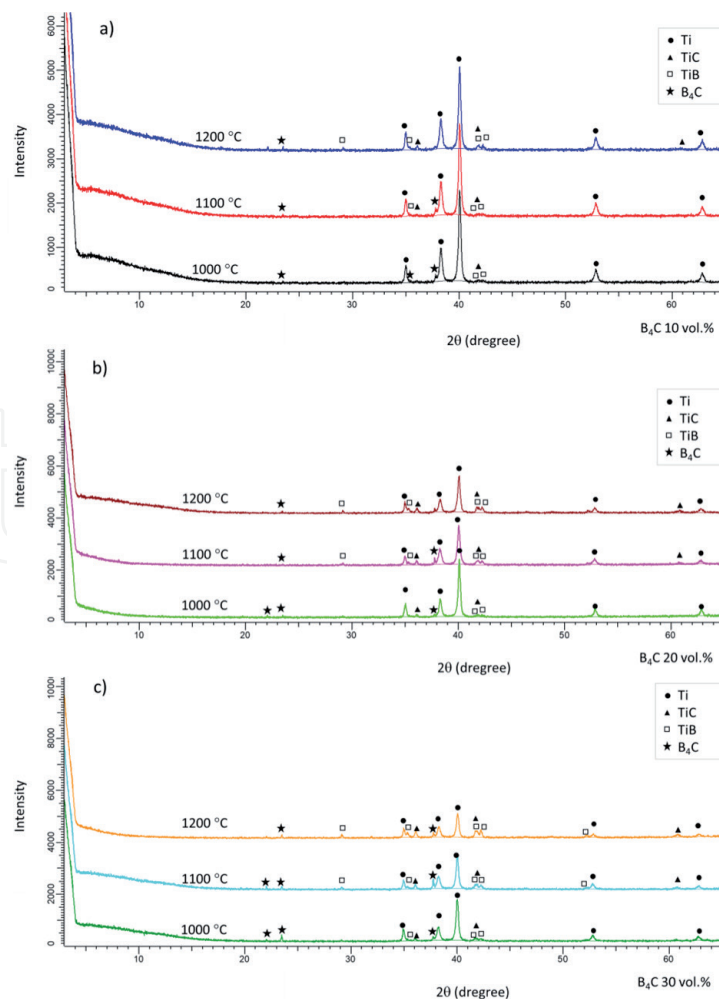


**Figure 10.** XRD patterns of TMCs reinforced in the starting blend with (a) 10 vol.% of B<sub>4</sub>C, (b) 20 vol.% of B<sub>4</sub>C, and (c) 30 vol.% of B<sub>4</sub>C.



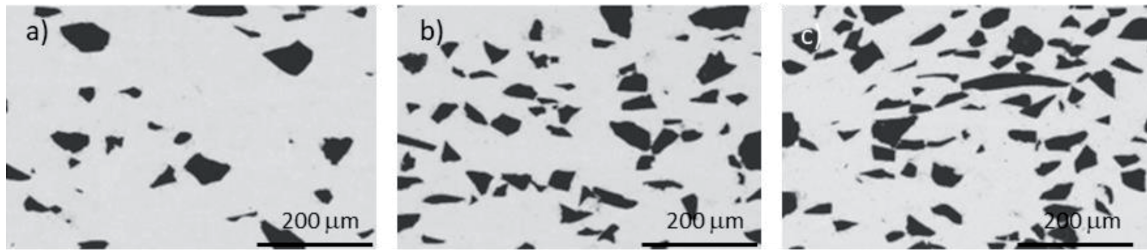


**Figure 11.** SEM images of TMCs produced at 1000°C with (a) 10 vol.% of  $B_4C$ , (b) 20 vol.% of  $B_4C$ , and (c) 30 vol.% of  $B_4C$ .

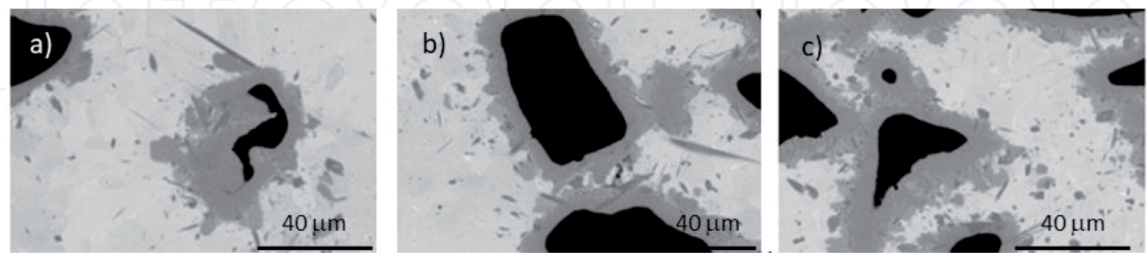


**Figure 12.** SEM images of TMCs produced at 1200°C with (a) 10 vol.%  $B_4C$ , (b) 20 vol.%  $B_4C$ , and (c) 30 vol.%  $B_4C$ .

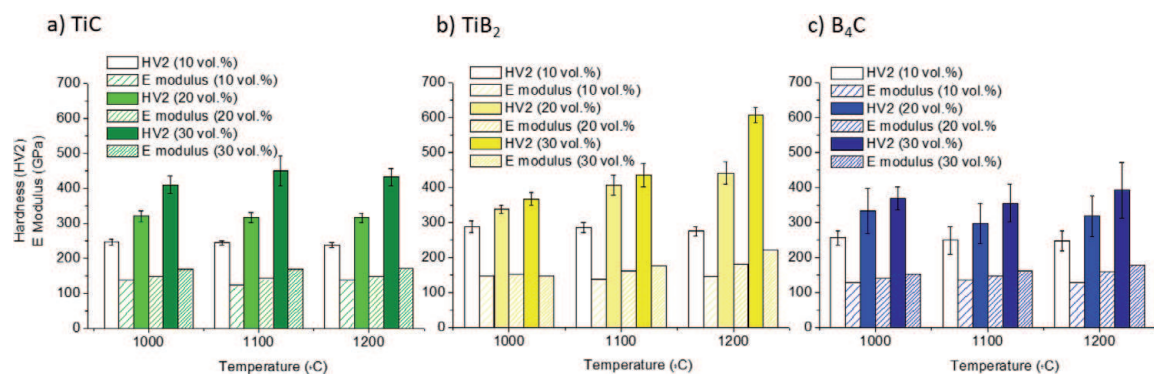


**Figure 13.** Hardness (HV2) and Young modulus values vs. operational temperature of the TMCs made from the different blends.

the formation of in situ phases. Regardless of the starting compositions, the morphologies of the in situ phases TiC and TiB are similar to the ones observed previously. On the one hand, there were precipitates with the particular whisker shape of TiB in the matrix. On the other hand, the presence of TiC can be seen as globular precipitated; both in situ phase morphologies have been wide and thoroughly studied [32].

### 3.2 Physical properties of the TMCs.

The relative density of the specimens was around 99.5% in the majority of the specimens, even in those whose microstructures had a few pores. It means that the processing parameters were suitable to achieve full densification.

As expected, the highest values of hardness and Young modulus were recorded in specimens whose starting blends were made from the highest ceramic particle contents. **Figure 13** shows a comparison of the hardness and Young modulus values of the TMCs produced at the three processing temperatures (1000, 1100, and 1200°C) and using the three compositions (10, 20, and 30 vol.%).

The operational temperature contributed to enhancing the hardness and the Young modulus; however, its influence varied depending on the type of ceramic particles employed in the starting blend, as reflected in **Figure 13**. TMCs reinforced by



TiB-TiB<sub>2</sub> phases showed the highest hardness measured. This development is closely related to the content of in situ formed TiB. Although there was also in situ formed TiB in TMCs made from blends with B<sub>4</sub>C particles, the maximum percentage formed (14 vol.%) in these specimens was lower than in TMCs made from the blend with TiB<sub>2</sub> (20 vol.%). In both cases, the TMCs were processed at 1200°C and 30 vol.%. In similar conditions, the highest Young modulus was also observed in TMCs reinforced with TiB-TiB<sub>2</sub> phases, in agreement with the commented results above.

In specimens made from blends with TiC, the main variation was only caused by the addition of more TiC content. Hardness and Young modulus values hardly increased by temperature, despite the diffusion of the C in the matrix and the TiC<sub>0.67</sub> formed.

Contrary to common thinking, the B<sub>4</sub>C reinforcement did not behave as the best precursor of in situ phases. Consequently, the expected properties may vary from the obtained values of hardness and Young modulus. The TiC and TiB formed were slightly lower than the in situ TiB formed in TMCs with TiB<sub>2</sub>. That means that the diffusion of B alone was major and the C could decelerate such diffusion. Furthermore, it should be highlighted that in specimens made from B<sub>4</sub>C, the values of hardness and Young modulus showed a wide standard deviation. This could be related to the in situ formed precipitates and their dispersion in the matrix.

#### 4. Conclusions

The conclusions of the current study which analyse the influence of the starting materials and operational temperature in the TMC properties are drawn:

- Reinforcing the titanium matrix with ceramic materials results in an enhancement of the TMC mechanical properties caused by the formation of in situ phases.
- XRD analysis states that the diffusion phenomenon of B and C elements into the matrix increases by the rising temperature; it is becoming increasingly important in the apparition of secondary phases.
- In evaluating the appropriateness of the operational parameters, the lower the temperature, the less the reactivity reinforcement matrix. This phenomenon was more significant when the concentration of reinforcement was the lowest one.
- The highest hardness and Young modulus of the TMCs were measured in specimens reinforced by TiB<sub>2</sub> particles.
- The densification of the specimens was achieved at the processing parameters tested.

#### Acknowledgements

The authors gratefully acknowledge the company “RHP-Technology GmbH” and the managers Dr. Neubauer and Dipl. Eng. Kitzmantel for their partial financial support of this work. In addition, the authors want to thank the Universidad de Sevilla for the use of experimental facilities at CITIUS Microscopy and X-Ray Laboratory Services (VI PPIT-2018-I.5 EVA MARÍA PÉREZ SORIANO).

## **Conflict of interest**

The authors declare no conflict of interest.

IntechOpen

IntechOpen

## **Author details**

Eva María Pérez-Soriano, Cristina M. Arévalo-Mora  
and Isabel Montealegre-Meléndez\*  
Universidad de Sevilla, Sevilla, Spain

\*Address all correspondence to: imontealegre@us.es

## **IntechOpen**

---

© 2019 The Author(s). Licensee IntechOpen. This chapter is distributed under the terms of the Creative Commons Attribution License (<http://creativecommons.org/licenses/by/3.0>), which permits unrestricted use, distribution, and reproduction in any medium, provided the original work is properly cited. 

## References

- [1] Chawla KK. Composite Materials: Science and Engineering. 2nd ed. New York: Springer; 2010. DOI: 10.1007/978-0-387-74365-3. 542 p
- [2] Tjong S, Ma Z. Microstructural and mechanical characteristics of in situ metal matrix composites. *Materials Science & Engineering R: Reports*. 2000;29(3):49-113. DOI: 10.1016/S0927-796X(00)00024-3
- [3] Lawrance GA. Front matter. In: Lawrance GA, editor. *Introduction to Coordination Chemistry*. Chichester: Wiley; 2010. pp. i-xix. DOI: 10.1002/9780470687123
- [4] Smith PR, Froes FH. Developments in titanium metal matrix composites. *Journal of Metals*. 1984;36(3):19-26. DOI: 10.1007/BF03338403
- [5] Leyens C, Peters M, editors. *Titanium and Titanium Alloys: Fundamentals and Applications*. 1st ed. Köln: Wiley; 2003. DOI: 10.1002/3527602119. 532 p
- [6] Kaczmar JW, Pietrzak K, Włosiński W. The production and application of metal matrix composite materials. *Journal of Materials Processing Technology*. 2000;106(1):58-67. DOI: 10.1016/S0924-0136(00)00639-7
- [7] Ranganath SA. Review on particulate-reinforced titanium matrix composites. *Journal of Materials Science*. 1997;32(1):1-16
- [8] Gofrey TMT, Goodwin PS, Ward-Close CM. Titanium particulate metal matrix composites: Reinforcement, production methods, and mechanical properties. *Advanced Engineering Materials*. 2000;2(3):85-91. DOI: 10.1002/(SICI)1527-2648(200003)2:3%3C85:AID-ADEM85%3E3.0.CO;2-U
- [9] Radhakrishna Bhat BV, Subramanyam J, Bhanu Prasad VV. Preparation of Ti-TiB-TiC & Ti-TiB composites by in-situ reaction hot pressing. *Materials Science and Engineering A*. 2002;325(1):126-130. DOI: 10.1016/S0921-5093(01)01412-5
- [10] Campbell FC. Metal matrix composites. In: Campbell FC, editor. *Manufacturing Technology for Aerospace Structural Materials*. Amsterdam: Elsevier Science; 2006. pp. 419-457. DOI: 10.1016/B978-1-85617-495-4.X5000-8
- [11] Montealegre Meléndez I, Neubauer E, Danninger H. Consolidation of titanium matrix composites to maximum density by different hot pressing techniques. *Materials Science and Engineering A*. 2010;527(16-17):4466-4473. DOI: 10.1016/j.msea.2010.03.093
- [12] Zhang C, Kong F, Xiao S, Niu H, Xu L, Chen Y. Evolution of microstructural characteristic and tensile properties during preparation of TiB/Ti composite sheet. *Materials and Design*. 2012;36:505-510. DOI: 10.1016/j.matdes.2011.11.060
- [13] Tjong SC, Mai YM. Processing-structure-property aspects of particulate- and whisker-reinforced titanium matrix composites. *Composites Science and Technology*. 2008;68(3-4):583-601. DOI: 10.1016/j.compscitech.2007.07.016
- [14] Zhang Z, Qin J, Zhang Z, Chen Y, Lu W, Zhang D. Microstructure effect on mechanical properties of in situ synthesized titanium matrix composites reinforced with TiB and La<sub>2</sub>O<sub>3</sub>. *Materials Letters*. 2010;64(3):361-363. DOI: 10.1016/j.matlet.2009.11.019
- [15] Xu D, Lu WJ, Yang ZF, Qin JN, Zhang D. In situ technique for synthesizing multiple ceramic particulates reinforced titanium

matrix composites (TiB+TiC+Y<sub>2</sub>O<sub>3</sub>)/Ti. *Journal of Alloys and Compounds*. 2005;**400**(1):216-221. DOI: 10.1016/j.jallcom.2005.04.018

[16] Ni DR, Geng L, Zhang J, Zheng ZZ. Effect of B<sub>4</sub>C particle size on microstructure of in situ titanium matrix composites prepared by reactive processing of Ti-B<sub>4</sub>C system. *Scripta Materialia*. 2006;**55**(5):429-432. DOI: 10.1016/j.scriptamat.2006.05.024

[17] Ma F, Lu W, Qin J, Zhang D, Ji B. Effect of forging and heat treatment on the microstructure of in situ TiC/Ti-1100 composites. *Journal of Alloys and Compounds*. 2007;**428**(1):332-337. DOI: 10.1016/j.jallcom.2006.03.060

[18] Zhang Y et al. Damping capacity of in situ TiB<sub>2</sub> particulates reinforced aluminium composites with Ti addition. *Materials and Design*. 2007;**28**(2): 628-632. DOI: 10.1016/j.matdes.2005.07.015

[19] Jimoh A. In-situ particulate-reinforcement of titanium matrix composites with borides [thesis]. Johannesburg: University of the Witwatersrand; 2010. Available from: <http://hdl.handle.net/10539/9323>

[20] Zhang Y, Sun J, Vilar R. Characterization of (TiB+TiC)/TC4 in situ titanium matrix composites prepared by laser direct deposition. *Journal of Materials Processing Technology*. 2011;**211**(4):597-601. DOI: 10.1016/j.jmatprotec.2010.11.009

[21] Jimoh A, Sigalas I, Hermann M. In situ synthesis of titanium matrix composite (Ti-TiB-TiC) through sintering of TiH<sub>2</sub>-B<sub>4</sub>C. *Materials Sciences and Applications*. 2012;**03**(01):30-35. DOI: 10.4236/msa.2012.31005

[22] Montealegre-Meléndez I, Neubauer E, Arévalo C, Rovira A, Kitzmantel M. Study of titanium metal matrix composites reinforced by boron

carbides and amorphous boron particles produced via direct hot pressing. *Key Engineering Materials*. 2016;**704**: 85-93. DOI: 10.4028/www.scientific.net/KEM.704.85

[23] Arévalo C, Kitzmantel M, Neubauer E, Montealegre-Meléndez I. Development of Ti-MMCs by the use of different reinforcements via conventional hot-pressing. *Key Engineering Materials*. 2016;**704**:400-405. DOI: 10.4028/www.scientific.net/KEM.704.400

[24] Arévalo C, Montealegre-Meléndez I, Ariza E, Kitzmantel M, Rubio-Escudero C, Neubauer E. Influence of sintering temperature on the microstructure and mechanical properties of In situ reinforced titanium composites by inductive hot pressing. *Materials*. 2016;**9**(11):919. DOI: 10.3390/ma9110919

[25] Neubauer E, Vály L, Kitzmantel M, Grech D, Ortega AR, Montealegre-Meléndez I, et al. Titanium matrix composites with high specific stiffness. *Key Engineering Materials*. 2016;**704**:38-43. DOI: 10.4028/www.scientific.net/KEM.704.38

[26] Montealegre-Meléndez I, Arévalo C, Perez-Soriano E, Neubauer E, Rubio-Escudero C, Kitzmantel M. Analysis of the influence of starting materials and processing conditions on the properties of W/Cu alloys. *Materials*. 2017;**10**(2): 142. DOI: 10.3390/ma10020142

[27] Ariza E, Montealegre-Meléndez I, Arévalo C, Kitzmantel M, Neubauer E. Ti/B<sub>4</sub>C composites prepared by in situ reaction using inductive hot pressing. *Key Engineering Materials*. 2017;**742**:121-128. DOI: 10.4028/www.scientific.net/KEM.742.121

[28] Montealegre-Meléndez I, Arévalo C, Pérez-Soriano EM, Kitzmantel M, Neubauer E. Microstructural and XRD analysis and study of the properties of the system Ti-TiAl-B<sub>4</sub>C processed

under different operational conditions.  
*Metals*. 2018;**8**(5):367. DOI: 10.3390/  
ma10111240

[29] Sabahi Namini A, Dilawary SAA, Motallebzadeh A, Shahedi Asl M. Effect of TiB<sub>2</sub> addition on the elevated temperature tribological behavior of spark plasma sintered Ti matrix composite. *Composites. Part B, Engineering*. 2019;**172**:271-280. DOI: 10.1016/j.compositesb.2019.05.073

[30] Ahmad A, Bond LJ, editors. *ASM Handbook. Nondestructive evaluation of materials*. 9th ed. Vol. 17. Ohio, United State of America; 1989

[31] Wang T, Gwalani B, Shukla S, Frank M, Mishra RS. Development of in situ composites via reactive friction stir processing of Ti–B<sub>4</sub>C system. *Composites. Part B, Engineering*. 2019;**172**:54-60. DOI: 10.1016/j.compositesb.2019.05.067

[32] Rielli VV, Amigó-Borrás V, Contieri RJ. Microstructural evolution and mechanical properties of in-situ as-cast beta titanium matrix composites. *Journal of Alloys and Compounds*. 2019;**778**:186-196. DOI: 10.1016/j.jallcom.2018.11.093